NRC·CNRC

NRC Publications Archive
Archives des publications du CNRC

Photophysical properties of dye-doped silica nanoparticles bearing different types of dye-silica interactions

Ma, Dongling; Kell, Arnold J.; Tan, Sophie; Jakubek, Zygmunt J.; Simard, Benoit

This publication could be one of several versions: author's original, accepted manuscript or the publisher's version. / La version de cette publication peut être l'une des suivantes : la version prépublication de l'auteur, la version acceptée du manuscrit ou la version de l'éditeur.
For the publisher's version, please access the DOI link below./ Pour consulter la version de l'éditeur, utilisez le lien DOI ci-dessous.

Publisher's version / Version de l'éditeur:
https://doi.org/10.1021/jp905812f
The Journal of Physical Chemistry C: Nanomaterials and Interfaces, 113, 36, pp. 15974-15981, 2009-08-01

NRC Publications Record / Notice d'Archives des publications de CNRC:
https://nrc-publications.canada.ca/eng/view/object/?id=17745c67-7bcd-486b-8b14-daecbc43474b
https://publications-cnrc.canada.ca/fra/voir/objet/?id=17745c67-7bcd-486b-8b14-daecbc43474b

Access and use of this website and the material on it are subject to the Terms and Conditions set forth at https://nrc-publications.canada.ca/eng/copyright
READ THESE TERMS AND CONDITIONS CAREFULLY BEFORE USING THIS WEBSITE.

L'accès à ce site Web et l'utilisation de son contenu sont assujettis aux conditions présentées dans le site https://publications-cnrc.canada.ca/fra/droits
LISEZ CES CONDITIONS ATTENTIVEMENT AVANT D'UTILISER CE SITE WEB.

Questions? Contact the NRC Publications Archive team at PublicationsArchive-ArchivesPublications@nrc-cnrc.gc.ca. If you wish to email the authors directly, please see the first page of the publication for their contact information.

Vous avez des questions? Nous pouvons vous aider. Pour communiquer directement avec un auteur, consultez la première page de la revue dans laquelle son article a été publié afin de trouver ses coordonnées. Si vous n'arrivez pas à les repérer, communiquez avec nous à PublicationsArchive-ArchivesPublications@nrc-cnrc.gc.ca.

National Research Council Canada | Conseil national de recherches Canada

Canada

Photophysical Properties of Dye-Doped Silica Nanoparticles Bearing Different Types of Dye−Silica Interactions

Dongling Ma,*,† Arnold J. Kell,‡ Sophie Tan,§ Zygmunt J. Jakubek,‡ and Benoit Simard*,‡

Institut National de la Recherche Scientifique, 1650 Boulevard Lionel-Boulet, Varennes, Quebec J3X 1S2, Canada, and Steacie Institute for Molecular Sciences, National Research Council of Canada, Ottawa, Ontario K1A 0R6, Canada

Received: June 20, 2009; Revised Manuscript Received: August 4, 2009

Photophysical properties of three types of dye-doped silica nanoparticles (NPs) with different dye−silica interactions have been investigated. In two cases the dye−silica interactions are noncovalent, where tris(2,2′-bipyridine)ruthenium(II) chloride (Rubpy) is attracted to the silica network electrostatically and tetramethylrhodamine-dextran (TMR-Dex) is trapped inside the silica matrix through spatial/steric hindrance. In the third case, tetramethylrhodamine-5-isothiocyanate (TRITC) modified with 3-aminopropyltriethoxysilane (APTES) to form TMR-APTES is bound to the silica matrix covalently. Although in all three types of architectures absorption, excitation, and emission spectra show only small red-shifts (<5 nm) as compared with free dye in water, excited state emission lifetimes, quantum yields, and anisotropies vary significantly and in quite different ways between the three architectures. All three types of interactions facilitate effective encapsulation of dye within a silica network. However, covalent bonding possesses a notable advantage over the other two types of interactions as it results in a large reduction of a nonradiative relaxation rate of the embedded dye (TMR-APTES) and, thus, a large (∼3.55-fold) increase of its quantum yield.

Introduction

High-sensitivity bioanalysis, rapid diagnostics, and effective therapeutics require the use of ultrabright and highly stable luminescent labels. Traditionally, organic fluorophores have been widely used as optical signaling biomarkers. However, they have suffered from some inherent, functional limitations. For example, most of them exhibit low signal intensities and undergo fast photobleaching.[1,2] Moreover, specific conjugation procedures normally need to be developed for different fluorophores. Luminescent nanoparticles (NPs) such as quantum dots (QDs) and dye-doped NPs hold great potential to overcome these limitations and serve as the next generation fluorescent probes. QDs are semiconductor nanocrystals (usually from 1 to 10 nm in diameter) and possess marked advantages of narrower emission, brighter luminescence, better long-term photostability, and broader excitation compared with conventional organic fluorophores.[3,4] Therefore, they promise to be used as excellent beacons after being tagged to biomolecules particularly for multiplex optical detection and long-term imaging.[5,6] However, for highly sensitive, demanding single biomolecular recognition event studies that require the observation of single probes, the power-law blinking behavior of individual QDs has been a big concern.[7,8] There is also concern over the safety of using heavy metal-based QDs for in vivo diagnostics due to their toxicity.[9] Dye-doped NPs, however, do not present such problems. Because each nanoparticle can contain thousands of dye molecules, it exhibits ensemble averaged behavior of multiple dye molecules. Also, in the case of the silica framework, they do not present the toxicity hazard. In this aspect, dye-doped NPs stand out as potentially superior fluorescent markers for single event studies.

Dye-doped NPs are made of nanosized organic or inorganic frameworks encapsulating multiple, up to ∼10 000, dye molecules. The luminous intensity of such NPs can be very high, in some cases exceeding that of QDs upon both one-photon and two-photon excitation.[10−13] As a consequence, ultrasensitive detection can be accomplished. For instance, an individual DNA hybridization event can be signaled by a large number of fluorophores contained in a single nanoparticle rather than by a single dye molecule attached to a DNA probe, resulting in much more intense signals.[14] Moreover, the solid matrix protects the dye molecules from quenchers such as oxygen and certain solutes in buffers, which likely results in more stable luminescence.[10,12,13,15]

Silica is the most commonly used inorganic shelling material as it has a number of advantages over organic as well as other inorganic materials.[16,17] In particular, silica-based NPs are resistant to microbial attack, stable in aqueous solutions, nontoxic, and biocompatible. In addition, they can be prepared easily with sizes smaller than those obtainable for polymer NPs. These features make them attractive for in vivo applications. Also, since silica surface modification and bioconjugation chemistry is well established, silica NPs can be easily conjugated with a variety of biomolecules for binding to targets with specificity and high affinity, both of which are typically required by biological applications.

Dyes can be encapsulated inside a silica matrix via various mechanisms such as electrostatic attraction, spatial constrain, or covalent bonding. However, the encapsulation can be experimentally challenging. Positively charged dye molecules are expected to have a high affinity to negatively charged silica surfaces and, consequently, be easily incorporated into silica framework from the reaction solution during nanoparticle formation.[18,19] However, Ogawa et al. have shown that such an electrostatic interaction is not very strong.[20] Doping hydrophobic

* To whom correspondence should be addressed. E-mail: benoit.simard@nrc-cnrc.gc.ca and ma@emt.inrs.ca.
† Institut National de la Recherche Scientifique.
‡ National Research Council of Canada.
§ Present address: Research & Development Center, Johnson & Johnson, Montreal, Quebec, Canada.

10.1021/jp905812f CCC: $40.75 © 2009 American Chemical Society
Published on Web 08/18/2009

CHART 1: Structures of Rubpy, Modified TMR for Conjugation with Dextran, and TMR-APTES

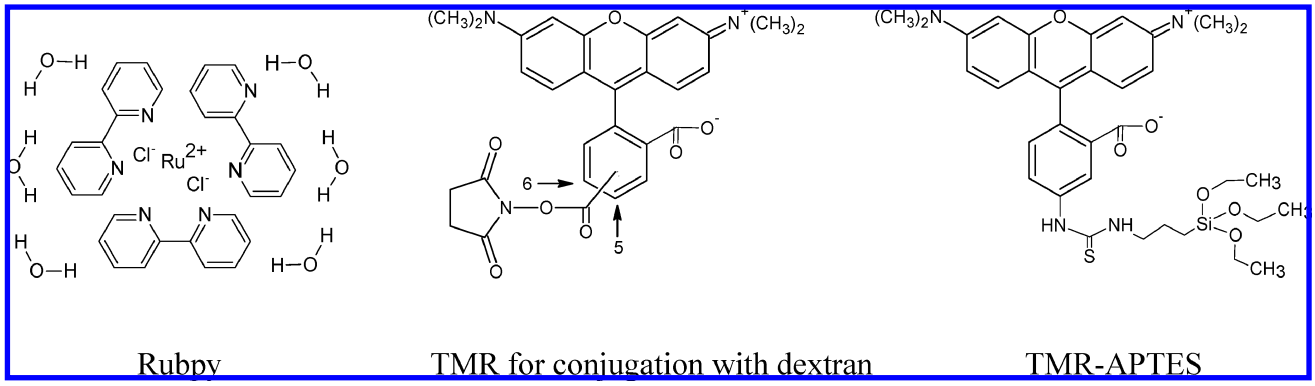

organic dyes into hydrophilic silica may pose a problem because of their limited solubility. The limitation can be overcome by first attaching water-soluble groups to dye molecules to increase the dye solubility in water and subsequently incorporating the modified dye molecules into a silica matrix through facile adsorption during nanoparticle synthesis.[21] Dye molecules can also be embedded into silica via formation of a covalent bond with a silane coupling agent, followed by co-condensation with tetraethoxysilane (TEOS).[22]

Dye-doped silica particles of different sizes, colors, and architectures have previously been synthesized through either an aqueous Stöber method or a reverse microemulsion method.[17−19] The Stöber method is simple, but often leads to formation of large, polydisperse NPs. In one example, large particles have been observed just 10 s after the reaction start and the authors have attributed the faster than expected growth to the change of the surface charge density due to the incorporation of positively charged dye molecules.[18] Uniform dye-doped particles with a diameter smaller than 100 nm have been prepared with the reverse microemulsion method. However, this method requires large amounts of surfactants and organic solvents and thus does not easily scale up.[23] Traditionally, it has been difficult to synthesize particles smaller than 30 nm by using either of these methods, though significant progress has been made very recently. Prasad's group has synthesized ultrasmall dye-doped NPs (~20 nm in diameter) using the Stöber method.[24] Similarly, Webb's group reported the synthesis of dye-doped silica particles with diameters of about 30 nm[25] and Wiesner's group created fluorescent silica-based nanoparticles with hydrodynamic diameters as small as 3.3 and 6.0 nm.[13] Both methods employ TEOS as the main construction material for silica nanoparticle framework. More recently, a one-pot synthesis of organosilica NPs using a single organosilicate with only three silanization groups was reported. The synthesis leads to formation of dye-doped silica NPs with inherently functionalized surface, in contrast to the silanol terminated NPs typically produced.[26]

Photophysical properties of dye-doped silica NPs have only been investigated to a limited extent. Zaccheroni et al. showed in their work that depending on the dye distribution in a silica network, dye molecules can exhibit either a monomeric or an excimer-like emission.[27] With a high dye concentration in solution during the doping process, the particles with core−shell structures can be formed. The heavily doped core shows the excimeric emission and the shell, where the concentration of dye molecules gradually decreases toward the surface, shows the monomeric emission. Webb et al. reported that by controlling the internal dye−silica architecture of particles, the photophysical behavior of dye molecules in silica can be manipulated.[25] Though these efforts survey the effect of dye−silica architectures on the optical properties of a specific dye, to the best of our knowledge there have not been any comparative studies of dye-doped silica NPs bearing different types of dye−silica interactions. Understanding how the bonding and spatial hindrance (related to the relatively small space of silica pores and interconnects, as compared with the size of dye molecules) affect the photophysical properties of dye molecules plays a fundamental role in designing new materials. Here we investigate the effects of dye−silica interaction on absorption, excitation, emission, emission lifetime, and emission anisotropy by synthesizing three types of dye-doped silica NPs in which dye molecules are embedded in silica networks either noncovalently or covalently. The dyes used in this work are tris(2,2′-bipyridine)ruthenium(II) chloride (Rubpy), tetramethylrhodamine-dextran (TMR-Dex), and tetramethylrhodamine-5-isothiocyanate (TRITC). Hereafter, we refer to the silica NPs doped with these dyes as Rubpy@SiO_2, TMR-Dex@SiO_2, and TMR-APTES@SiO_2, where TMR-APTES designates the reaction product of TRITC and 3-aminopropyltriethoxysilane (APTES). The chemical structures of Rubpy, modified tetramethylrohdamine (TMR) used by the supplier to conjugate with dextran, and TMR-APTES are shown in Chart 1. Due to the complexity of the structure of dextran that is a high-molecular-weight branched polymer made of glucose we do not show its structure here.

Experimental Section

Chemicals. Rubpy was purchased from Alfa Aesar, Johnson Matthey Company. TRITC and TMR-Dex (M_w = 10 000) were both acquired from Invitrogen Canada. TEOS and APTES (99+%) were obtained from Gelest. Ammonium hydroxide (NH_4OH, 28−30 wt %) and high purity 2-propanol were both obtained from EMD Chemicals. Triton X-100, cyclohexane, hexyl alcohol, *N*,*N*-dimethylformamide (DMF), and ethanol were purchased from Sigma-Aldrich, BDH, Anachemia Canada, EM Science, and Commercial Alcohols, respectively. All chemicals were used as purchased. Throughout the preparation, purified water (18 MΩ cm) was used exclusively. Water was purified with use of a Millipore Q-guard 2 purification system (Millipore Corporation).

Synthesis of Rubpy@SiO_2 NPs. Rubpy-doped silica NPs were prepared via a reverse microemulsion method.[17] The synthesis of the silica NPs and the Rubpy doping process were accomplished simultaneously in a microemulsion. The water-in-oil microemulsion was prepared by mixing 1.8 mL of Triton X-100, 7.5 mL of cyclohexane, 1.8 mL of hexyl alcohol, and 340 μL of water. Then, 774 μL of Rubpy water solution (10.3 mg/mL) was added to the microemulsion, which was sonicated to aid the rapid formation of a uniform dispersion. Subsequently,

100 μL of TEOS and 60 μL of NH_4OH were added. The molar ratio of TEOS to Rubpy was ~40:1. The reaction was run for over 24 h in an aluminum foil-covered reactor and then terminated by adding acetone. The Rubpy@SiO_2 NPs were collected by centrifugation and washed with water and ethanol to remove unreacted reagents. The purified luminescent NPs were then dispersed in water for characterization.

Synthesis of TMR-Dex@SiO_2 NPs. TMR-Dex doped silica NPs were prepared in a similar way as Rubpy@SiO_2.[21] First, TMR-Dex was dissolved in diluted hydrochloric acid (pH 1.5−1.6) to form a TMR-Dex aqueous solution of 10 mg/mL. Next, the water-in-oil microemulsion was prepared by mixing 1.8 mL of Triton X-100, 7.5 mL of cyclohexane, 1.8 mL of hexyl alcohol, and 480 μL of the TMR-Dex solution followed by the addition of 100 μL of TEOS. NH_4OH (60 μL) was added 30 min later to accelerate silica polymerization. The molar ratio of TEOS to TMR-Dex was ~930:1 in the reaction solution. The reaction was run for 24 h in an aluminum foil-covered reactor and quenched by the addition of acetone. Finally, the NPs were collected by centrifugation and washed several times with water and ethanol to remove unreacted reagents. The purified NPs were then dispersed in water for characterization.

Synthesis of TMR-APTES@SiO_2 NPs. The synthesis of TMR-APTES@SiO_2 NPs was done in two steps. First, TRITC was covalently linked with APTES to form TMR-APTES, a dye−silane conjugate, which in the second step reacted with the main silica building material TEOS to realize the encapsulation. To form the covalent linkage, 0.4 mg of TRITC was dissolved in 0.5 mL of DMF, to which 5 μL of a 1:10 APTES solution in DMF was added. The mixture was vortexed overnight and used immediately the next day. To achieve the encapsulation, 0.4 μL of the TRITC-APTES solution was mixed with 17 mL of anhydrous ethanol and 1.28 mL of NH_4OH. After shaking for 15 min, 20 μL of TEOS was added and the mixture was continuously shaken for 18 h. The TEOS/TMR-APTES molar ratio was ~125 000:1 in the reaction solution. Finally, the NPs were collected by centrifugation and washed several times with water to remove unreacted reagents. The purified NPs were then dispersed in water for characterization.

Characterization. Transmission electron microscopy (TEM) images of the NPs were acquired with a Philips CM20 FEG microscope operating at 200 kV. The samples were prepared by depositing a droplet of the nanoparticle dispersion onto TEM grids. For photophysical characterization, all samples were dispersed in water. UV−visible absorption spectra were recorded on a Varian Cary 5000 UV−vis−NIR spectrophotometer. Excitation, emission, emission lifetime, and emission anisotropy measurements were all performed with a Horiba Jobin Yvon Fluorolog Tau-3 Lifetime System. Excitation spectra were taken at emission wavelength of 608 nm for Rubpy and 578 nm for TMR-Dex and TMR-APTES samples. Emission spectra were recorded with an excitation wavelength of 450 nm for Rubpy and 550 nm for both TMR-Dex and TMR-APTES samples. For emission lifetime and emission anisotropy measurements, all the samples tested were adjusted to have the absorbance of 0.1 or less at the wavelength of interest. The lifetimes were measured employing a frequency domain method. In this method, continuous excitation light is modulated at various frequencies resulting in modulated emission with a modulation amplitude and a modulation phase both depending on sample lifetimes. The modulation phase and modulation amplitude were recorded at a series of modulation frequencies and lifetimes were obtained by fitting both sets of data to appropriate decay models. In the emission anisotropy measurements Rubpy samples were excited at 450 nm and TMR-Dex and TMR-APTES samples at 550 nm.

Results and Discussion

In the present study of effects of silica−dye interaction on photophysical properties of dye molecules embedded in silica NPs, all dyes were loaded into silica at low concentrations (i.e., high TEOS/dye molar ratios in doping solutions) to avoid or minimize dye aggregation during silica encapsulation.[28−30] The actual, experimentally optimized, ratio varied from ~40:1 for Rubpy, through ~930:1 for TMR-Dex, to ~125 000:1 for TMR-APTES reflecting the effectiveness of encapsulation and/or strength of dye−silica interaction on going from Rubpy to TMR-Dex and to TMR-APTES.

The three types of dye-doped silica NPs were synthesized by using either the reverse microemulsion or the Stöber method. While Rubpy, as a cationic dye, directly encapsulated within the silica network via electrostatic attraction, noncovalent and covalent encapsulation of TMR molecules involved a more complex procedure. TMR is a hydrophobic dye and is not soluble in water. Therefore, to embed it into hydrophilic silica, in one case a conjugate of TMR and Dextran, which is water-soluble and thus compatible with the sol−gel process, was used. Dextran, as determined by ζ-potential measurements, is weakly negatively charged over a wide range of solution pH. Since silica is also negatively charged, an acidic synthetic environment via addition of hydrochloric acid was applied in order to minimize electrostatic repulsion between TMR-Dex and silica and promote incorporation of the dye in the early stage of nucleation and growth of NPs.[21] After particle synthesis and redispersion in water at neutral pH, TMR-Dex molecules remained trapped inside silica pores. The relatively small size of the silica pores and interconnects as compared with the size of dextran polymer molecules hindered diffusion of polymer (and hence TMR) molecules out of the silica network. In addition to facilitating encapsulation of the TMR fluorophores within the silica network and preventing leaching, the dextran backbone also acted as a spacer between TMR fluorophores limiting dye aggregation even at high loadings.[21] In another case, TMR fluorophores were covalently linked to silica. TMR molecules bearing isothiocyanate groups (i.e., TRITC) were reacted with APTES silane molecules to generate TMR-APTES precursors, which were co-condensed with TEOS to form TMR-APTES-doped silica NPs.

Together, these synthetic protocols facilitated investigation of electrostatic (Rubpy), steric (TMR-Dex), and covalent (TMR-APTES) interactions of dye molecules with silica networks. Two of the dye molecules studied here, Rubpy and TMR-APTES, have comparable molecular weights (MW: 749 and 665, respectively). The third one, TMR-Dex, is much larger (MW: 10 000) with most of the molecular weight contributed by the dextran polymer.

Panels a−c of Figure 1 show TEM images of the silica NPs doped with Rubpy, TMR-Dex, and TMR-APTES, respectively. In all three cases, NPs appear to be spherical or slightly oval and have sizes larger than 40 nm in diameter. The reason to choose to work with over-40 nm nanoparticles in this study is to minimize the relative contribution of surface effects to the overall photophysical properties of dye-doped silica NPs. All resulting particles are dispersible in water.

The UV−vis absorption spectra of free dye molecules and dye-doped SiO_2 NPs were measured in aqueous solutions (Figure 2A). Both free Rubpy molecules and Rubpy@SiO_2 NPs showed a similar broad absorption band with the characteristic

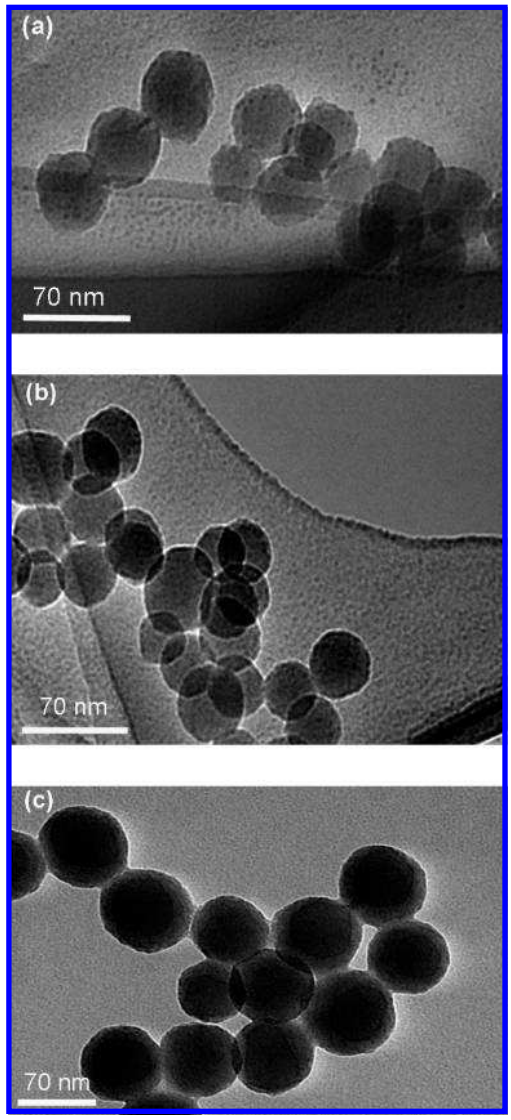

Figure 1. TEM images of (a) Rubpy@SiO_2, (b) TMR-Dex@SiO_2, and (c) TMR-APTES@SiO_2 NPs.

absorption peak red-shifted by ~5 nm for the latter. Free TMR-Dex molecules displayed two prominent absorption maxima at 517 and 554 nm attributed to dimeric and monomeric species, respectively. The presence of dimeric (or multimeric) species in rhodamine and its derivatives at high concentrations has previously been reported by Levy et al.[31,32] Silica encapsulation red-shifted the maxima by ~2 nm and changed the intensity ratio of the two peaks ($A_{517/554}$ from ~1.6 to ~1.3). Silica-encapsulated TMR-APTES molecules displayed primarily monomeric absorption red-shifted by ~5 nm with a rather small dimer contribution ($A_{515/554} = 0.4$). The results suggested that the low-concentration dye encapsulation process did not lead to an increased rate of dimerization as compared with free dye in solution. The small red shifts observed in the absorption spectra of the three types of dye-doped NPs indicated that the encapsulated dye molecules were located in a slightly more polar environment than free dyes in water.[33]

Like the absorption spectra, the excitation and emission spectra of all three dye-doped silica NPs (Figure 2B−D) have not changed much (peak shifts <5 nm) as compared to those of free dye molecules. It is noteworthy that the excitation spectra of TMR-Dex and TMR-Dex@SiO_2 do not display the prominent peak at 517 nm, indicating that the dimeric species do not contribute to the emission at 578 nm. Among the three types of structures, TMR-Dex shows the largest peak shifts upon silica encapsulation, a ~5 nm red shift from 548 to 553 nm in the excitation spectrum and an ~3.5 nm red shift from 572.5 to 576 nm in the emission spectrum. However, the excitation and emission spectra of the free and silica encapsulated TMR-Dex dye look essentially identical, suggesting that there is little interaction between the dye molecules within the silica matrix.

Emission of dye molecules is usually affected by the polarity of its environment. For example, Handa et al. has found that Rubpy in a nonionic water-in-oil microemulsion shows two peaks in its emission spectrum: the one at a shorter wavelength (582.5 nm) is due to Rubpy in a less polar environment while the one at a longer wavelength (615 nm) is due to dye molecules in a more polar environment in the microemulsion.[34] Montalti et al. has found that when polarity-sensitive dansyl dye molecules are encapsulated within silica NPs of increasingly larger diameters their emission maxima can blue shift by as much as 40 nm.[35] They proposed that this shift is due to a polarity difference between the silica matrix and the bulk solvent. Moreover, it was found that dye molecules included in the more isolated core region emitted at more blue-shifted wavelengths as compared to those situated near the surface of spherical particles, where the environment was more polar because of solvent penetration. Aside from medium polarity, specific dye−solvent interactions (e.g., coordination) also shift emission spectra.[33] Thus, it appears that variation of emission spectra mirrors variation of the local environment around dye molecules.[29] It is clear that in all three cases studied here, the encapsulation process only weakly affects the photoluminescence spectra of the dye molecules. This observation was further supported by an investigation of the emission spectra of Rubpy and TMR-Dex doped NPs with significantly different diameters, which showed no NP-size dependence of the spectra. The relatively small shifts (no more than 5 nm) observed in the spectra of fluorophores following encapsulation indicate rather small variation of the local dye environment (e.g., local polarity) within the silica matrix as compared to aqueous solution. This is likely due to the solvent permeation into the silica.

Montalti et al. estimated the thickness of a water-permeable silica layer to be from 3 to 4 nm, regardless of the nanoparticle size.[35] However, Ow et al. claimed that their dye doped NPs were impermeable to a solvent.[11] Both findings may be correct as the solvent permeability of a silica network is determined by the network's morphology, which, in turn, is controlled by synthesis parameters. Even though the entire volume of our NPs is likely accessible to water and thus local environments sensed by a dye molecule in silica and a solution are similar, a notable difference is that the silica network effectively protects dye molecules against photodegradation.[12,13,15] We observed that under the same strong illumination conditions free Rubpy loses over 40% of its initial emission intensity, while the emission intensity of Rubpy@SiO_2 only drops by less than 5% after 250 min of continuous illumination.

Emission of dye molecules is also sensitive to the concentration of dye molecules inside a silica matrix.[28,29] For example, in highly doped silica NPs, the excited pyrene dye molecules interact with ground-state ones, leading to a formation of excimers which are responsible for the appearance of a broad emission band at longer wavelengths as compared to the monomeric emission band.[27] Similar phenomena have been reported for dye molecules belonging to the rhodamine family.[31] In our study no excimer emission was observed for either TMR-Dex or TMR-APTES, the rhodamine family architectures. In

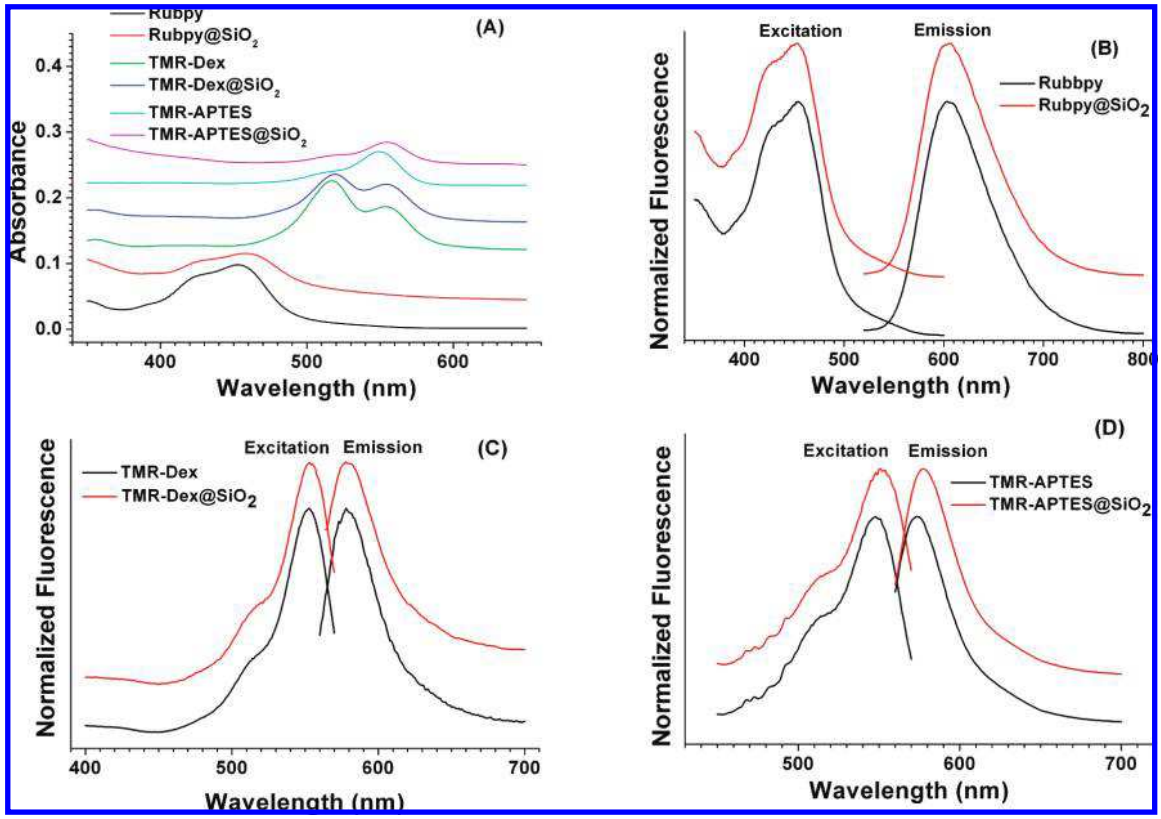

Figure 2. (A) Absorption spectra of Rubpy, TMR-Dex, and TMR-APTES free dyes and the corresponding dye-doped silica NPs in water. Excitation and emission spectra of (B) Rubpy and Rubpy@SiO_2, (C) TMR-Dex and TMR-Dex@SiO_2, and (D) TMR-APTES and TMR-APTES@SiO_2. The spectra were displaced vertically to avoid overlap. Excitation spectra were taken at emission wavelength of 608 nm for Rubpy and 578 nm for TMR-Dex and TMR-APTES samples. Emission spectra were recorded with excitation wavelength of 450 nm for Rubpy and 550 nm for both TMR-Dex and TMR-APTES samples.

TABLE 1: Emission Lifetime, Relative Quantum Yield, and Emission Anisotropy of Dyes and Dye-Doped Silica NPs

	Rubpy	Rubpy@SiO_2	TMR-Dex	TMR-Dex@SiO_2	TMR-APTES	TMR-APTES@SiO_2
τ_1[a] (ns)	359 (1)	377 (1)	2.06 (6)	1.5 (1)	1.94 (6)	3.67 (6)
	15 (5)	62.9 (1)				
Φ_{rel}[b]	1		1.3		3.55	
α[c]	0.000 (5)	0.019 (5)	0.08 (1)	0.21 (1)	0.02 (1)	0.29 (2)

[a] τ: lifetime; the second line entry, when present, is a width of the lifetime distribution. [b] Φ_{rel}: relative quantum yield of silica encapsulated dye as compared with free dye in water. [c] α: anisotropy.

addition, we observed that, with a relatively low dye loading, the fluorescence quantum yield of Rubpy remained unchanged following silica encapsulation.[36] However, it should be noted that at high loadings dye molecules such as Rubpy can self-quench, resulting in a quantum yield reduction.[29,30,37,38] The quantum yields of silica encapsulated TMR-Dex and TMR-APTES were determined to be ~1.3 and 3.55 times higher than quantum yields of the TMR-Dex and TMR-APTES molecules in water, respectively. The effect of silica encapsulation on the quantum yield of the three dyes will be discussed in detail below.

The effect of silica encapsulation on the emission lifetime and anisotropy widely varies among the three nanoparticle architectures prepared in this study (Table 1). The fluorescence intensity decay for TMR-Dex and TMR-APTES molecules in water could be best fit by a single exponential function yielding 2.06 ± 0.06 and 1.94 ± 0.06 ns for their excited state lifetime, respectively (Figure 3). Although fluorescence intensity decay for free Rubpy in water could also acceptably be fitted to a single exponential function resulting in a lifetime estimate of 358 ± 1 ns, a fit with a Lorentzian distribution of lifetimes with the average lifetime of $\tau = 359 \pm 1$ ns and the distribution width of $\Delta\tau = 15 \pm 5$ ns was statistically more rigorous. The fluorescence decay of Rubpy@SiO_2 was similarly modeled by using the Lorentzian lifetime distribution yielding $\tau = 377 \pm 1$ and $\Delta\tau = 62.9 \pm 0.1$ ns. Statistically equivalent fit was obtained with a double-exponential model yielding the major lifetime component $\tau_1 = 323 \pm 2$ ns; $f_1 = 0.76$ and the minor component $\tau_2 = 633 \pm 10$ ns; $f_2 = 0.14$, where f_1 and f_2 are fractional contributions of two lifetimes. Santra et al. have correlated two lifetimes observed for fluorescein isothiocyanate doped silica NPs with two different microenvironments, which are associated with different solvation conditions, around dye molecules.[39] A similar phenomenon has also been reported for 1,1′-diethyl-3,3,3′,3′-tetramethylindocarbocyanine iodide doped mesoporous silica nanoparticles.[30] Since the absorption and fluorescence spectra of our Rubpy@SiO_2 NPs do not indicate that Rubpy resides in two significantly different environments within the silica matrix, we prefer the single component Lorentzian distribution of lifetimes model. However, we should point out that the excited state lifetime is much more sensitive to variations in the local environment than the absorption and emission spectra and a small variation in the strength of Rubpy−silica interactions within the NPs undetectable by the absorption and emission spectra could still result in a splitting of the lifetime.

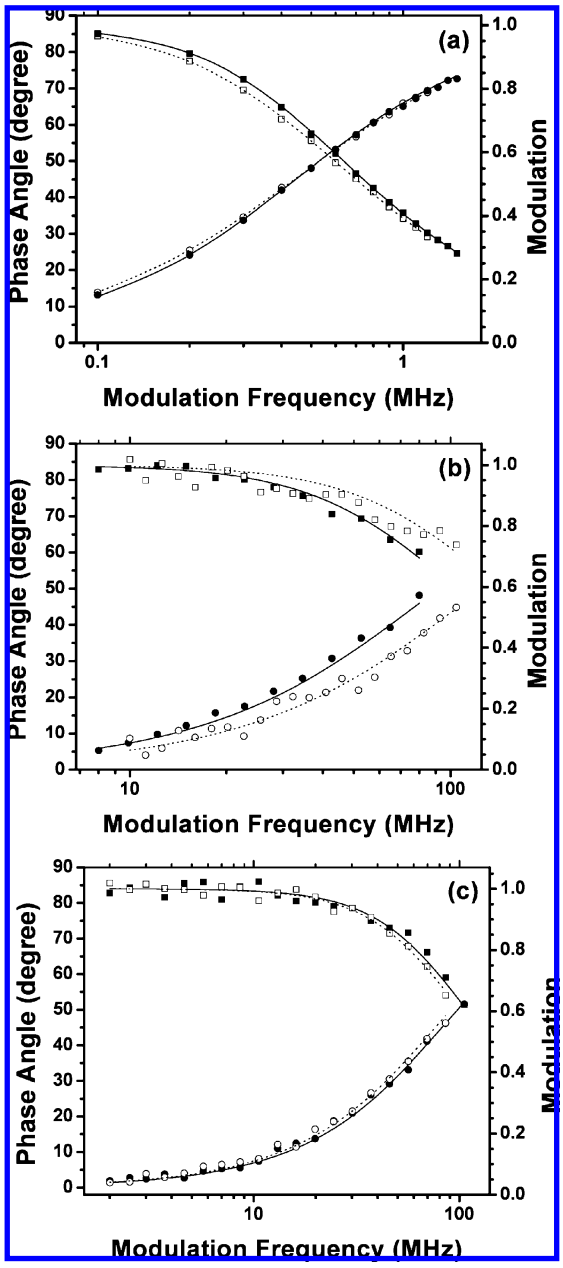

Figure 3. Simulated frequency-domain data for (a) Rubpy and Rubpy@SiO_2, (b) TMR-Dex and TMR-Dex@SiO_2, and (c) TMR-APTES and TMR-APTES@SiO_2: (●) phase angle of free dye molecules, (○) phase angle of dye-doped silica NPs, (■) modulation of free dye molecules, (□) modulation of dye-doped silica NPs, and (—) fit.

Due to the fluctuation of charge amount or density on silica walls, the electrostatic attraction between individual Rubpy molecules and silica may vary, which, in turn, can modify the radiative and/or nonradiative rates resulting in broadening of the lifetime distribution or lifetime splitting. Two TMR derivatives show large and opposite change of lifetime following their encapsulation into the silica matrix. For TMR-Dex, we observe a lifetime decrease from 2.06(6) to 1.5(1) ns whereas for TMR-APTES we observe an increase from 1.94(6) to 3.67(6) ns. The increase of dye lifetime after silica encapsulation has also been reported by others.[15,25]

The emission anisotropy of Rubpy shows a small, but statistically significant, increase (from 0.000(5) to 0.019(5)) in the main emission band from 570 to 650 nm following silica encapsulation (Table 1). Because Rubpy is highly symmetrical, its fundamental anisotropy is small ($r_0 \approx 0.1$). The near-zero measured steady-state anisotropy of free Rubpy molecules as well as the small value for Rubpy@SiO_2 can be easily understood by considering its small molecular size (thus rapid rotation) and relatively long emission lifetime. The small increase of anisotropy upon silica encapsulation indicates that the motion of Rubpy molecules in the silica network is somewhat restricted. It may also include a contribution resulting from breaking the molecular symmetry of Rubpy in an inhomogeneous silica environment. Measured emission anisotropy of TMR-Dex and TMR-APTES increases more prominently after silica encapsulation from 0.08(1) to 0.21(1) and from 0.02(1) to 0.29(2), respectively. This suggests that the rotational motion of both encapsulated dye molecules is severely restricted.[40] Previously, Larson et al. proposed that decreased mobility limits intramolecular rotation modes, causing the reduction of deactivation modes and thus decreasing nonradiative rate.[25] Because our NPs are similar to those reported by Larson et. al, we expect the nonradiative rate for both TMR-Dex@SiO_2 and TMR-APTES@SiO_2 to decrease as well.

An excited state lifetime, τ, and a quantum yield, Φ, can be expressed in terms of radiative and nonradiative decay rates as:

$$\tau = 1/(k_r + k_{nr}) \quad (1)$$

and

$$\Phi = k_r/(k_r + k_{nr}) \quad (2)$$

By combining eqs 1 and 2, the radiative and nonradiative rates can be respectively expressed as:

$$k_r = \Phi/\tau \quad (3)$$

and

$$k_{nr} = (1 - \Phi)/\tau \quad (4)$$

Since we are interested in effects of silica encapsulation on properties of dyes as compared with free dye molecules in water, we rewrite eqs 3 and 4 as relative rates

$$k_{r,rel} = k_{r,s}/k_{r,f} = (\Phi_s/\Phi_f)/(\tau_s/\tau_f) = \Phi_{rel}/\tau_{rel} \quad (5)$$

and

$$k_{nr,rel} = k_{nr,s}/k_{nr,f} = (1 - \Phi_s)/(1 - \Phi_f)/(\tau_s/\tau_f) = (1 - \Phi_f\Phi_{rel})/(1 - \Phi_f)/\tau_{rel} \quad (6)$$

where the subscripts s and f indicate values for encapsulated and free dye molecules in water, respectively, Φ_{rel} is a relative quantum yield, and τ_{rel} is a relative lifetime.

Recalling that the quantum yield of Rubpy does not change upon silica encapsulation, we observe that the radiative rate changes proportionally to the lifetime change and estimate $k_{r,\,rel} = 1.05$. The radiative rate of silica excapsulated TMR-Dex (TMR-Dex@SiO_2) is estimated to be ~1.78 times greater than that for free TMR-Dex. Similarly, silica encapsulation of TMR-APTES leads to an increase of the radiative rate by a

factor of 1.88. The radiative rate increase upon silica encapsulation observed here for TMR-Dex and TMR-APTES is not unusual as a 2-fold enhancement of the radiative rate has previously been reported for rhodamine dyes.[25]

Discussion of the relative nonradiative rate is more complicated, since, as evident from eq 6, it requires knowledge of an absolute quantum yield of free dye molecules or, alternatively, molecules embedded in silica NPs. Therefore, we measured the quantum yield of TMR-Dex in water to be 0.10 with reference to the quantum yield of TRITC in water.[41] For TMR-APTES we used the quantum yield value of 0.14 previously determined by Soper et al. for a similar TMR derivative.[41] With these values we calculated quantum yields for TMR-Dex@SiO_2 and TMR-APTES@SiO_2 to be equal to 0.13 and 0.50, respectively. Subsequently, we estimated that silica encapsulation leads to an increase of the nonradiative rate of TMR-Dex by a factor of 1.3 and a decrease of the nonradiative rate for TMR-APTES by a factor of 3.2. While the nonradiative rate decreased as expected for TMR-APTES,[25] its increase for TMR-Dex upon silica encapsulation was somewhat surprising. However, the increased rate for TMR-Dex can be rationalized by enhanced, as compared with solution, quenching of the excited state by vibrational modes of dextran chains, leading to a sufficient increase of the nonradiative rate to overcompensate the reduction of the rate due to the restriction of the TMR-Dex motion.

Conclusions

Three types of dye-doped silica NPs—Rubpy@SiO_2, TMR-Dex@SiO_2, and TMR-APTES@SiO_2—have been synthesized. These architectures have facilitated investigation of effects of electrostatic interaction (Rubpy), steric hindrance (TMR-Dex), and covalent bonding (TMR-APTES) on photophysical properties of dyes encapsulated within a silica nanoparticle matrix. To ensure dye−dye interaction within a silica matrix to be negligible, low-concentration dye doping has been applied. This strategy has simplified the complexity of the studied systems and allowed for direct correlation of variation in the fundamental photophysical behavior with dye−silica interaction.

We have found that in all three cases silica encapsulation only weakly affects absorption, excitation, and emission spectra. However, the emission lifetime, quantum yield, and steady-state emission anisotropy of the studied dye molecules vary considerably depending on how the dye is encapsulated within the silica. For Rubpy, broadening of the lifetime distribution indicates the presence of an inhomogeneous microenvironment in silica. The rather small increase of the measured emission anisotropy and average lifetime suggests weak interaction of Rubpy with the silica host material. The excited state lifetime of TMR-Dex decreases while the measured anisotropy increases considerably and both the lifetime and anisotropy of TMR-APTES significantly increase following silica encapsulation. The large increase of measured emission anisotropy indicates that motion of both TMR-Dex and TMR-APTES in silica is strongly restricted. The radiative rate of both TMR-Dex and TMR-APTES slightly increases upon silica encapsulation, by a factor 1.78 and 1.88, respectively. Dramatically different, however, is the effect of encapsulation on the nonradiative rate, which increases by a factor of 1.3 for TMR-Dex, but decreases by a factor of 3.2 for TMR-APTES. Our investigation shows that in all three cases dye molecules are effectively confined within a silica network with varying effect of the matrix on the photophysical properties of a dye. The covalent bonding of dye molecules with a silica network is a preferred method of encapsulation as it strongly enhances quantum yield by suppressing nonradiative relaxation. While steric hindrance also leads to an increase of the dye quantum yield, the increase is rather small as, presumably, the presence of long polymeric chains in the vicinity of a silica encapsulated dye molecule strongly enhances nonradiative relaxation largely reducing an opposite and desired effect of restriction of motion.

Acknowledgment. Financial support from CBRN Research and Technology Initiative (CRTI) 03-0005RD and 06-0187TD is greatly appreciated. Financial support from the Natural Sciences and Engineering Research Council of Canada and Fonds de la recherche sur la nature et les technologies is also greatly appreciated.

References and Notes

(1) Zhou, X.; Zhou, J. *Anal. Chem.* **2004**, *76*, 5302.
(2) Fare, T. L.; Coffey, E. M.; Dai, H. Y.; He, Y. D.; Kessler, D. A.; Kilian, K. A.; Koch, J. E.; LeProust, E.; Marton, M. J.; Meyer, M. R.; Stoughton, R. B.; Tokiwa, G. Y.; Wang, Y. *Anal. Chem.* **2003**, *75*, 4672.
(3) Chan, W. C. W.; Nie, S. *Science* **1998**, *281*, 2016.
(4) Michalet, X.; Pinaud, F. F.; Bentolila, L. A.; Tsay, J. M.; Doose, S.; Li, J. J.; Sundaresan, G.; Wu, A. M.; Gambhir, S. S.; Weiss, S. *Science* **2005**, *307*, 538.
(5) Yezhelyev, M. V.; Al-Hajj, A.; Morris, C.; Marcus, A. I.; Liu, T.; Lewis, M.; Cohen, C.; Zrazhevskiy, P.; Simons, J. W.; Rogatko, A.; Nie, S.; Gao, X.; O'Regan, R. M. *Adv. Mater.* **2007**, *19*, 3146.
(6) Bouzigues, C.; Morel, M.; Triller, A.; Dahan, M. *Proc. Natl. Acad. Sci. U.S.A.* **2007**, *104*, 11251.
(7) Durisic, N.; Bachir, A. I.; Kolin, D. L.; Hebert, B.; Lagerholm, B. C.; Grutter, P.; Wiseman, P. W. *Biophys. J.* **2007**, *93*, 1338.
(8) Jaiswal, J. K.; Simon, S. M. *Trends Cell Biol.* **2004**, *14*, 497.
(9) Michalet, X.; Pinaud, F. F.; Bentolila, L. A.; Tsay, J. M.; Doose, S.; Li, J. J.; Sundaresan, G.; Wu, A. M.; Gambhir, S. S.; Weiss, S. *Science* **2005**, *307*, 538.
(10) Wang, L.; Wang, K.; Santra, S.; Zhao, X.; Hilliard, L. R.; Smith, J. E.; Wu, Y.; Tan, W. *Anal. Chem.* **2006**, *78*, 647.
(11) Ow, H.; Larson, D. R.; Srivastava, M.; Baird, B. A.; Webb, W. W.; Wiesner, U. *Nano Lett.* **2005**, *5*, 113.
(12) Nakamura, M.; Ishimura, K. *J. Phys. Chem. C* **2007**, *111*, 18892.
(13) Burns, A. A.; Vider, J.; Ow, H.; Herz, E.; Penate-Medina, O.; Baumgart, M.; Larson, S. M.; Wiesner, U.; Bradbury, M. *Nano Lett.* **2009**, *9*, 442.
(14) Zhou, X.; Zhou, J. *Anal. Chem.* **2004**, *76*, 5302.
(15) Lal, M.; Levy, L.; Kim, K. S.; He, G. S.; Wang, X.; Min, Y. H.; Pakatchi, S.; Prasad, P. N. *Chem. Mater.* **2000**, *12*, 2632.
(16) Jain, T. K.; Roy, I.; De, T. K.; Maitra, A. *J. Am. Chem. Soc.* **1998**, *120*, 11092.
(17) Santra, S.; Zhang, P.; Wang, K.; Tapec, R.; Tan, W. *Anal. Chem.* **2001**, *73*, 4988.
(18) Shibata, S.; Taniguchi, T.; Yano, T.; Yamane, M. *J. Sol-Gel Sci. Technol.* **1997**, *10*, 263.
(19) Grasset, F.; Dorson, F.; Cordier, S.; Molard, Y.; Perrin, C.; Marie, A. M.; Sasaki, T.; Haneda, H.; Bando, Y.; Mortier, M. *Adv. Mater.* **2008**, *20*, 143.
(20) Ogawa, M.; Nakamura, T.; Mori, J.; Kuroda, K. *J. Phys. Chem. B* **2000**, *104*, 8554.
(21) Zhao, X.; Bagwe, R. P.; Tan, W. *Adv. Mater.* **2004**, *16*, 173.
(22) Blaaderen, A. V.; Vrij, A. *Langmuir* **1992**, *8*, 2921.
(23) Rossi, L. M.; Shi, L.; Quina, F. H.; Rosenzweig, Z. *Langmuir* **2005**, *21*, 4277.
(24) Kumar, R.; Roy, I.; Ohulchanskyy, T. Y.; Goswami, L. N.; Bonoiu, A. C.; Bergey, E. J.; Tramposch, K. M.; Maitra, A.; Prasad, P. N. *ACS Nano* **2008**, *2*, 449.
(25) Larson, D. R.; Ow, H.; Vishwasrao, H. D.; Heikal, A. A.; Wiesner, U.; Webb, W. W. *Chem. Mater.* **2008**, *20*, 2677.
(26) Nakamura, M.; Ishimura, K. *Langmuir* **2008**, *24*, 5099.
(27) Rampazzo, E.; Bonacchi, S.; Montalti, M.; Prodi, L.; Zaccheroni, N. *J. Am. Chem. Soc.* **2007**, *129*, 14251.
(28) Malfatti, L.; Kidchob, T.; Aiello, D.; Aiello, R.; Testa, F.; Innocenzi, P. *J. Phys. Chem. C* **2008**, *112*, 16225.
(29) Imhof, A.; Megens, M.; Engelberts, J. J.; de Lang, D. T. N.; Sprik, R.; Vos, W. L. *J. Phys. Chem. B* **1999**, *103*, 1408.

(30) Gianotti, E.; Bertolino, C. A.; Benzi, C.; Nicotra, G.; Caputo, G.; Castino, R.; Isidoro, C.; Coluccia, S. *ACS Appl. Mater. Interface* **2009**, *1*, 678.
(31) Monte, F. D.; Mackenzie, J. D.; Levy, D. *Langmuir* **2000**, *16*, 7377.
(32) Marme, N.; Friedrich, A.; Denapaite, D.; Hakenbeck, R.; Knemeyer, J. *Chem. Phys. Lett.* **2006**, *428*, 440.
(33) Fodor, L.; Lendvay, G.; Horváth, A. *J. Phys. Chem. A* **2007**, *111*, 12891.
(34) Handa, T.; Sakai, M.; Nakagaki, M. *J. Phys. Chem.* **1986**, *90*, 3377.
(35) Montalti, M.; Prodi, L.; Zaccheroni, N.; Battistini, G.; Marcuz, S.; Mancin, F.; Rampazzo, E.; Tonellato, U. *Langmuir* **2006**, *22*, 5877.
(36) Ma, D.; Jakubek, Z. J.; Simard, B. *J. Nanosci. Nanotechnol.* **2006**, *6*, 3677.
(37) Ogawa, M.; Nakamura, T.; Mori, J.; Kuroda, K. *J. Phys. Chem. B* **2000**, *104*, 8554.
(38) Santra, S.; Wang, K.; Tapec, R.; Tan, W. *J. Biomed. Opt.* **2001**, *6*, 160.
(39) Santra, S.; Liesenfeld, B.; Bertolino, C.; Dutta, D.; Cao, Z.; Tan, W.; Moudgil, B. M.; Mericle, R. A. *J. Lumin.* **2006**, *117*, 75.
(40) Tleugabulova, D.; Duft, A. M.; Brook, M. A.; Brennan, J. D. *Langmuir* **2004**, *20*, 101.
(41) Soper, S. A.; Nutter, H. L.; Keller, R. A.; Davis, L. M.; Shera, E. B. *Photochem. Photobiol.* **1993**, *57*, 972.

JP905812F